Effect of a nucleating agent on lamellar growth in melt-crystallizing polyethylene oxide Effect of a nucleating agent on lamellar growth in melt-crystallizing polyethylene oxide

ARTICLE *in* JOURNAL OF APPLIED PHYSICS · MAY 2003

Impact Factor: 2.18 · DOI: 10.1063/1.1564877 · Source: arXiv

4 AUTHORS, INCLUDING:

Francesco Aliotta
Italian National Research Council
116 PUBLICATIONS **1,017** CITATIONS
SEE PROFILE

M. Pieruccini
Italian National Research Council
55 PUBLICATIONS **353** CITATIONS
SEE PROFILE

AIP | Journal of Applied Physics

Effect of a nucleating agent on lamellar growth in melt-crystallizing polyethylene oxide

F. Aliotta, G. Di Marco, R. Ober, and M. Pieruccini

Citation: J. Appl. Phys. **93**, 5839 (2003); doi: 10.1063/1.1564877
View online: http://dx.doi.org/10.1063/1.1564877
View Table of Contents: http://jap.aip.org/resource/1/JAPIAU/v93/i9
Published by the American Institute of Physics.

Effect of a nucleating agent on lamellar growth in melt-crystallizing polyethylene oxide

F. Aliotta and G. Di Marco
C.N.R. Istituto per i Processi Chimico-Fisici, Sezionne di Messina, Via La Farina 237, I-98123 Messina, Italy

R. Ober
Laboratoire de Physique de la Matiere Condensee, C.N.R.S. URA 792, College de France; 11, Place Marcelin Berthelot, F-75231 Paris Cedex, France

M. Pieruccini[a)]
C.N.R. Istituto per i Processi Chimico-Fisici, Sezionne di Messina, Via La Farina 237, I-98123 Messina, Italy

(Received 22 April 2002; accepted 10 February 2003)

The effects of a (non co-crystallizing) nucleating agent on secondary nucleation rate and final lamellar thickness in isothermally melt-crystallizing polyethylene oxide are considered. Small angle x-ray scattering reveals that lamellae formed in nucleated samples are thinner than in the pure samples crystallized at the same undercoolings. These results are in quantitative agreement with growth rate data obtained by calorimetry, and are interpreted as the effect of a local decrease of the basal surface tension, determined mainly by the nucleant molecules diffused out of the regions being about to crystallize. Quantitative agreement with a simple lattice model allows for some interpretation of the mechanism. © *2003 American Institute of Physics.*
[DOI: 10.1063/1.1564877]

Nucleating agents have important applications in the industrial use of polymeric materials. As an example, mechanical properties such as hardness and elastic moduli can be controlled with these additives, which are able to affect crystallization kinetics rather dramatically.[1] In fact, not only the *primary* nucleation rate is influenced, but also the lamellar growth process via *secondary* nucleation. In the context of bulk crystallization, the latter mechanism has been envisaged for the first time within the framework of a phenomenological interpretation of the free growth kinetics' data of indigo-nucleated isotactic polypropylene.[2,3] Later, similar observations in nucleated high density polyethylene and polyethylene oxide (PEO) have been interpreted in the same way, with the further support of lattice calculations for the basal lamellar interface.[4]

The basic idea is that during growth, the nucleant molecules present in regions which are about to crystallize, diffuse towards the forming basal interfaces prior to crystallization (in all the cases above, the nucleating agent did not co-crystallize). These molecules cause a local decrease of the basal surface tension σ_e, so they tend to remain confined in the interfacial regions because diffusion towards the amorphous bulk would require an extra energy to restore a higher value of σ_e. In this situation the linear growth velocity v in low to moderate undercooled melts is still related to the secondary nucleation free enthalpy ΔG by[5]

$$v \propto \exp\{-\Delta G/kT\} \tag{1}$$

(with T the temperature), but the expression

$$\sigma_e = \sigma_{e0}\left(1 + \frac{a}{\Delta T}\right) \tag{2}$$

has to be substituted for σ_{e0} in the formula

$$\Delta G = 4 b_0 \sigma \sigma_{e0} \frac{v_c T_m}{H_f \Delta T} \tag{3}$$

customarily used for pure systems. In the above Eqs. (2) and (3), b_0 is the stem diameter, σ is the lateral surface tension, σ_{e0} is the basal surface tension in the absence of the nucleant, T_m is the equilibrium melting point, H_f/v_c is the enthalpy of fusion per unit volume, $\Delta T = T_m - T$, and a (<0) is a coefficient proportional to the concentration of nucleating agent[2–4] (see below).

Figure 1 shows the overall crystallization rates obtained by accurate differential scanning colorimetry (DSC) measurements on PEO nucleated with a number density $n \cong 2.6 \times 10^{19}$ cm^{-3} of indigo (i.e., 1% wt fraction) in the interval $331 \leqslant T \leqslant 334$ K.[4] Fittings with Eqs. (1)–(3) are also reported for the cases where either a is let free to change, or is set equal to zero. Assuming $T_m = 338$ K, the best fit is found with $a \cong -1.8$ K; besides, a close value for this parameter (-1.7 K) can be calculated by means of a simple lattice model.[4]

Consider now the morphological features controlled by the nucleant in *crystallized* PEO. At fixed ΔT, the number and final size of the spherulites are influenced by indigo through the primary nucleation rate. About the role played by secondary nucleation, Eq. (2) is of relevance. Since the lamellar fold length is related to σ_e by

$$l = 2\sigma_e \frac{v_c T_m}{H_f \Delta T}, \tag{4}$$

a)Electronic mail: pierucci@me.cnr.it

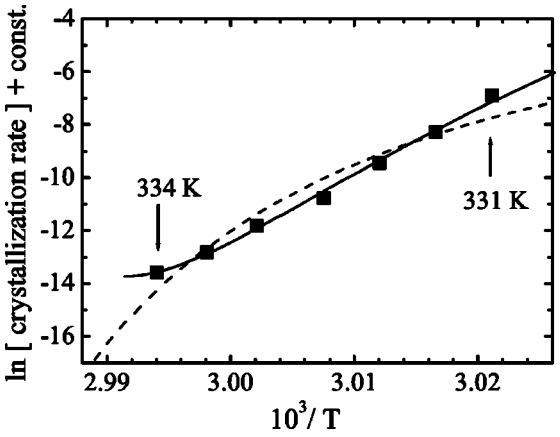

FIG. 1. Logarithm of the crystallization rate (approximately $\ln v^2$) as a function of T^{-1} for PEO nucleated with a number density $n=2.6\times10^{19}\mathrm{cm}^{-3}$ of indigo; the dashed line is a best fit using Eqs. (1) and (3); the solid line is obtained after substitution of σ_{e0} with Eq. (2).

it is expected that the lamellar thickness of nucleated samples should be smaller than in pure samples crystallized at the same ΔT, and for $|a/\Delta T|$ not too large:

$$\frac{l_0-l}{l_0}\cong-\frac{a}{\Delta T}, \tag{5}$$

where l_0 is given by Eqs. (2) and (4) with $a=0$.

Small angle x-ray scattering (SAXS) measurements carried out on pure and nucleated PEO (with the same content of indigo as for the case of Fig. 1) in fact confirm this prediction.

To assure homogeneity, nucleated samples were prepared from a solution of PEO 600 000 (Aldrich) and the appropriate amount of indigo in acetonitrile, which was kept under stirring for one day. The solvent was then very slowly evaporated at about 50 C. Pure PEO samples were prepared with a similar procedure. Before crystallization, the samples were kept above the melting temperature for half an hour or more, and then cooled as rapidly as possible to the preset crystallization temperature.

The SAXS measurement apparatus consists of a Rigaku rotating anode generator, with a wavelength of 1.54 Å. The counter was 76 cm from the sample and the dimension of the beam at the counter was 3×0.5 mm^2, so that desmearing was necessary (point collimation measurements, with a 0.5×0.5 mm^2 beam, were performed as a check, and gave the same results, although with relatively less statistics). All measurements have been carried out at room temperature.

The lamellar thicknesses in the pure (l_0) and nucleated (l) samples have been estimated from the evaluation of the interface distribution function $K''(s)$;[6,7] the results are reported in Table I. The relatively small electron density difference between amorphous and crystalline regions in PEO rendered the data analysis a bit cumbersome. The spurious background forward scattering characterizing these systems (which is not unusual in general[8]) was modeled by a *local* (i.e., $q=0$) Gaussian distribution of density fluctuations, whose amplitude and width [the latter always found in the range $(4.5–7.5)\times10^{-3}$ Å^{-1}] were obtained by means of best fitting procedures. Figure 2 shows the interface distributions $K''(s)$ for some of the PEO samples. The first maximum in $K''(s)$ is assigned to the interlamellar thickness, since (i) its position is weakly dependent on ΔT, as can be deduced from Table I, and (ii) the linear crystallinity thus found gets closer to the DSC one ($\approx65\%$ at a rate -1 C/min in both nucleated and pure PEO). The resulting Gibbs–Thomson plot is in Fig. 3. The linear fit to the pure PEO data points extrapolates to a melting temperature $T_m^\infty=339.3$ K, i.e., rather close to the above value of T_m. Moreover, assuming $H_f/v_c\cong210$ J cm^{-3},[9,10] a surface tension $\sigma_{e0}\approx70$ erg cm^{-2} is found (cf. also Ref. 10).

TABLE I. SAXS results for long period and lamellar thickness at room temperature in pure (L_0 and l_0) and nucleated (L and l) PEO, all in Å, isothermally crystallized at the undercoolings ΔT. The estimates of $-a/\Delta T$ are obtained from SAXS, best fit in Fig. 1 (Cal.) and lattice calculations with $\sigma_{e0}=20$ erg cm^{-2} (Lat$_1$) and $\sigma_{e0}=70$ erg cm^{-2} (Lat$_2$).

ΔT	L_0	l_0	L	l	$-a/\Delta T$			
					SAXS	Cal.	Lat$_1$	Lat$_2$
7.3	330	250	260	180	0.28	0.25	0.24	0.17
9.7	285	215	250	180	0.16	0.18	0.17	0.12
10.3	290	220	240	175	0.2	0.17	0.16	0.11
11.3	280	210	240	170	0.14	0.16	0.15	0.11
14.6	230	160				0.12	0.12	0.09
16	215	145	210	140	0.03	0.11	0.11	0.08
19.8	180	110				0.09	0.09	0.06

As the crystallization temperature decreased, complete thermalization was ever more difficult to achieve in PEO/indigo samples before the onset of crystallization. For nucleated samples crystallized at large ΔT the preset temperature was only apparent. For example, at $T=322$ K (i.e., $\Delta T=16$ K in Table I) the lamellar thickness of the pure and nucleated samples almost coincide, although a 0.1 relative difference had to be expected.

The ratio $-a/\Delta T$ as obtained from SAXS, fitting of the data in Fig. 1 (Cal.), and from lattice calculations, is also reported in Table I. The good agreement between the values of this parameter as obtained by SAXS (*grown* lamellae) and best fitting (*growing* lamellae), indicates that in the present T

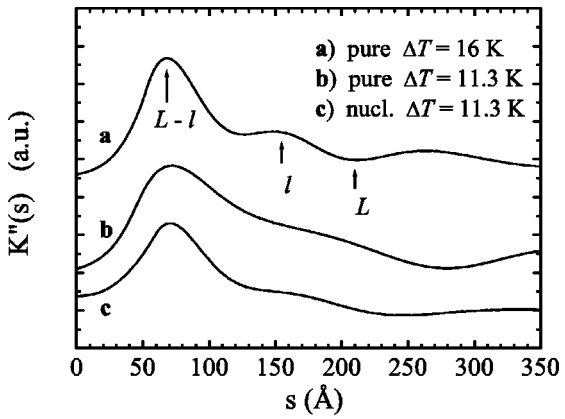

FIG. 2. Comparison between interface distances distribution functions at room temperature, $K''(s)$, of pure and nucleated PEO samples crystallized at different ΔT's. L and l are the long period and the lamellar thickness, respectively.

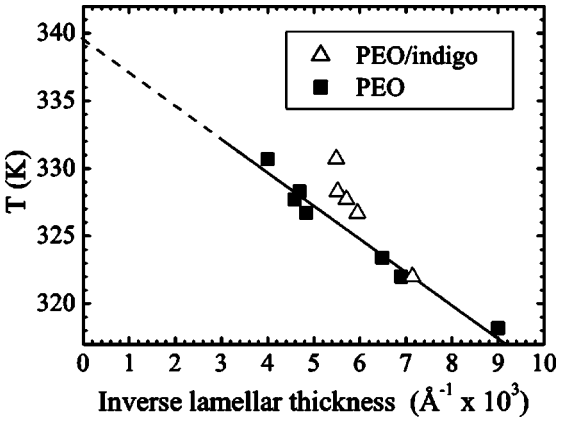

FIG. 3. Inverse lamellar thickness as a function of the crystallization temperature for pure and nucleated PEO from SAXS.

range the mechanism described by Eq. (2) plays a main role in the influence of the nucleant on the growth process. Moreover, it supports the hypothesis that the nucleant remains confined at the basal interfaces during lamellar growth, without appreciable increase of the nucleant concentration in the remaining amorphous phase.

Some insight into the underlying mechanism can be gained from the lattice description.[4] In the crystalline region the chain segment fractional occupation of the lattice sites is $\phi_c=1$, and the orientational entropy associated to bonds connecting adjacent segments in the chain is lowest. On the other hand, in the amorphous bulk the fractional occupation ϕ_a (i.e., the amorphous-to-crystalline density ratio) is less than ϕ_c, and is related to an appropriate Flory–Huggins segment/vacuum interaction parameter χ_{p0} ($=1.8$ for PEO); correspondingly, the bond orientational entropy is highest. In the interfacial region the fractional occupation ϕ is higher than ϕ_a, i.e., the chain segments are somewhat compressed, while a relatively large bond orientational entropy is still maintained. This contributes to the overall σ_e. Now, when a nucleant molecule is put in place of a segment in a site adjoining the folding plane, then (i) a nucleant/segment solvation energy arises, which is described by a parameter χ_s ($\leqslant 0$), (ii) a local segment–segment compression work correspondingly disappears and (iii) steric hindrance causes a decrease in the bond orientational entropy associated to the neighboring chain segments. All these issues contribute to the change in σ_e. From the analytic expression of σ_e the following approximation can be found,[11] showing explicitly the three contributions above:

$$\left(\frac{d\sigma_e}{d\varphi}\right)_{n=0} \approx \frac{kT}{b_0^2}\left[(\chi_s-\chi_{p0})-\frac{1}{2}-\ln\left(\frac{z}{2}\right)\right], \tag{6}$$

where z ($=6$) is the lattice coordination number and φ is the average number of nucleant molecules diffusing out of the volume of a forming stem, towards *one* of the ends of the stem itself ($\varphi \cong n b_0^2 l_0/2$ for given ΔT).

Two important facts need be stressed. The first is that $(\partial\sigma_e/\partial\varphi)_{n=0}$ turns out to be weakly dependent on χ_s:[4] a reasonable range for the latter, within which any value can be taken, is $0>\chi_s>-0.5$ (the lower bound corresponding to a "solvation energy" of ≈ 1.3 kJ/mol). The second is that $(\partial\sigma_e/\partial\varphi)_{n=0}$ is independent of σ_{e0} in this (rough) approximation; in fact, from the expression[4]

$$a \cong n b_0^2 T_m \frac{v_c}{H_f}\left(\frac{\partial\sigma_e}{\partial\varphi}\right)_{n=0}, \tag{7}$$

full calculations yield $a\cong -1.7$ K for $\sigma_{e0}=20$ erg cm^{-2},[9] or $a\cong -1.2$ K for $\sigma_{e0}\approx 70$ erg cm^{-2}. These values can be compared with $a\cong -0.7$ K as obtained from Eq. (6). In Table I the resulting $-a/\Delta T$ for both these σ_{e0} values are reported.

In summary, we have shown that in the present case Eq. (2) is supported by growth kinetics' data, SAXS, and lattice calculations. Moreover, a microscopic picture of the mechanism, as well as an approximate expression for the coefficient a, is provided by the lattice model.

[1] H. E. Bair, in *Thermal Characterization of Polymeric Materials*, edited by E. A. Turi (Academic, San Diego, 1981).
[2] M. Pieruccini, G. Di Marco, and M. Lanza, J. Appl. Phys. **80**, 1851 (1996).
[3] M. Pieruccini, J. Appl. Phys. **81**, 2995 (1997).
[4] F. Aliotta, G. Di Marco, and M. Pieruccini, Physica A **298**, 266 (2001).
[5] E. J. Donth, *Relaxation and Thermodynamics in Polymers* (Akademie, Berlin, 1992).
[6] W. Ruland, Colloid Polym. Sci. **255**, 417 (1977).
[7] J. Schmidtke, G. Strobl, and T. Thurn-Albercht, Macromolecules **30**, 5804 (1997).
[8] Z.-G. Wang, B. S. Hsiao, and N. Sanjeeva Murthy, J. Appl. Crystallogr. **33**, 690 (2000).
[9] Yu. Godowsky and G. L. Slonimsky, J. Polym. Sci. **12**, 1053 (1974).
[10] K. Mezghani and P. J. Phillips, in *Physical Properties of Polymers Handbook*, edited by J. E. Mark (AIP, New York, 1996).
[11] Equation (6) can be obtained from the full expression of σ_e, Eq. (19) in Ref. 4, considering that the fractional site occupation ϕ in the layer adjoining the folding plane is decreased by the fractional site occupation φ of the nucleant in such a way that $\phi+\varphi\approx$const., with $\varphi \ll \phi \approx 1$, without changing significantly the number of tight folds, Fig. 2 in Ref. 4, and finally considering that the segment chemical potential at constant ϕ, Eq. (16) in Ref. 4, does not change significantly throughout the basal interphase.